Bioorganic & Medicinal Chemistry 21 (2013) 186–195

Contents lists available at SciVerse ScienceDirect

Bioorganic & Medicinal Chemistry

journal homepage: www.elsevier.com/locate/bmc

Synthesis and biological evaluation of novel propargyl amines as potential fluorine-18 labeled radioligands for detection of MAO-B activity

S. Nag [a,*], G. Kettschau [b], T. Heinrich [b], A. Varrone [a], L. Lehmann [b], B. Gulyas [a], A. Thiele [b], É. Keller [c], C. Halldin [a]

[a] Karolinska Institutet, Department of Clinical Neuroscience, Psychiatry Section, Karolinska Hospital, S-17176, Stockholm, Sweden
[b] Bayer HealthCare AG, Global Drug Discovery, Berlin, Germany
[c] Semmelweis University, Department of Forensic and Insurance Medicine, H-1450 Budapest, Hungary

ARTICLE INFO

Article history:
Received 31 July 2012
Revised 20 October 2012
Accepted 25 October 2012
Available online 15 November 2012

Keywords:
Monoamine oxidase (MAO)
PET
Monkey
Human
Autoradiography
Fluorine-18
Kinetics
Metabolites

ABSTRACT

The aim of this project was to synthesize and evaluate three novel fluorine-18 labeled derivatives of propargyl amine as potential PET radioligands to visualize monoamine oxidase B (MAO-B) activity.

The three fluorinated derivatives of propargyl amine ((*S*)-1-fluoro-*N*,4-dimethyl-*N*-(prop-2-ynyl)-pent-4-en-2-amine (**5**), (*S*)-*N*-(1-fluoro-3-(furan-2-yl)propan-2-yl)-*N*-methylprop-2-yn-1-amine (**10**) and (*S*)-1-fluoro-*N*,4-dimethyl-*N*-(prop-2-ynyl)pentan-2-amine (**15**)) were synthesized in multi-step organic syntheses. IC_{50} values for inhibition were determined for compounds **5**, **10** and **15** in order to determine their specificity for binding to MAO-B. Compound **5** inhibited MAO-B with an IC_{50} of 664 ± 48.08 nM. No further investigation was carried out with this compound. Compound **10** inhibited MAO-B with an IC_{50} of 208.5 ± 13.44 nM and compound **15** featured an IC_{50} of 131.5 ± 0.71 nM for its MAO-B inhibitory activity. None of the compounds inhibited MAO-A activity (IC_{50} > 2 μM).

The fluorine-18 labeled analogues of the two higher binding affinity compounds (**10** and **15**) (*S*)-*N*-(1-[^{18}F]fluoro-3-(furan-2-yl)propan-2-yl)-*N*-methylprop-2-yn-1-amine (**16**) and (*S*)-1-[^{18}F]fluoro-*N*,4-dimethyl-*N*-(prop-2-ynyl)pentan-2-amine (**18**) were both prepared from the corresponding precursors **9A, 9B** and **14A, 14B** by a one-step fluorine-18 nucleophilic substitution reaction. Autoradiography experiments on human postmortem brain tissue sections were performed with **16** and **18**. Only compound **18** demonstrated a high selectivity for MAO-B over MAO-A and was, therefore, chosen for further examination by PET in a cynomolgus monkey.

The initial uptake of **18** in the monkey brain was 250% SUV at 4 min post injection. The highest uptake of radioactivity was observed in the striatum and thalamus, regions with high MAO-B activity, whereas lower levels of radioactivity were detected in the cortex and cerebellum. The percentage of unchanged radioligand **18** was 30% in plasma at 90 min post injection.

In conclusion, compound **18** is a selective inhibitor of MAO-B in vitro and demonstrated a MAO-B specific binding pattern in vivo by PET in monkey. It can, therefore, be considered as a candidate for further investigation in human by PET.

1. Introduction

Monoamine oxidase (MAO), a flavin adenine dinucleotide (FAD) containing enzyme is important for regulating the levels of monoaminergic neurotransmitters and of bioactive monoamines by catalyzing their deamination.[1] Two MAO isozymes such as MAO-A and MAO-B, are distinguished by substrates specificity, inhibitor selectivity and amino acid sequences.[2] MAO-A catalyzes the oxidation of for example 5-hydroxytryptamine (5-HT) and norephinephrine and is inhibited by low concentrations (nM) of clorgyline and pirlindole whereas MAO-B catalyzes the oxidation of for example benzyl amine and is inhibited by (*R*)-deprenyl and rasagiline in nanomolar concentrations. MAO inhibitors are used for the treatment of psychiatric and neurological disorders. MAO-A inhibitors are prescribed mainly for depression[3] and MAO-B inhibitors are mostly used for the treatment of Parkinson's disease (PD)[4] as well as depression.[5] Therefore, MAO inhibitors have attracted significant attention for further research. Previous

Abbreviations: PET, positron emission tomography; MAO, monoamino oxidase; MAOI, monoamino oxidase inhibitor; PD, Parkinson's disease; AD, Alzheimer's disease; NMR, Nuclear magnetic resonance; UPLC, Ultra performance liquid chromatograpy; HPLC, High performance liquid chromatography; LC, Liquid chromatography; LC–MS, Liquid chromatography–Mass spectrometry; DMSO, dimethylsulfoxide; DMF, dimethylformamide; PBS, phosphate buffered solution; IC, inhibitory concentration; ARG, autoradiography; SUV, standard uptake value; ROI, region of interest.

* Corresponding author. Tel.: +46 8 51775018.
E-mail address: sangram.nag@ki.se (S. Nag).

0968-0896/$ - see front matter © 2012 Elsevier Ltd. All rights reserved.
http://dx.doi.org/10.1016/j.bmc.2012.10.050

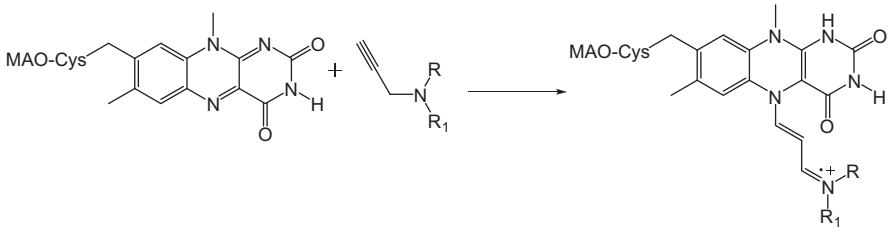

Figure 1. Proposed mechanism of inactivation of MAO by propargylamine derivatives.

research shows that the flavoprotein MAO-B can irreversibly be inactivated by propargylamine derivatives.[5] The mechanism is illustrated in Figure 1. In which the oxidized propargylamine derivative to the corresponding highly electrophilic eyniminium species by MAO binds to the flavin group with covalent bond forming an adduct leading to inactivation of the enzyme by micromolar concentrations.

Positron emission tomography (PET) is a non-invasive imaging technique which has widely been utilized to visualize the localization of MAO-B in monkey and human brain. Imaging brain MAO-B activity by employing [^{11}C]deuterated deprenyl as ligand with PET in humans has been useful for studying neurodegenerative diseases[6,7] and epilepsy.[8] In recent years several propargylamine derivatives have been labeled with carbon-11 and fluorine-18 to be applied as PET radioligands such as [^{11}C]pargyline,[9] [^{11}C]L-deprenyl,[10] [^{11}C]deuterium-L-deprenyl,[11] [^{11}C]SL25.1188,[12] DL-4-[^{18}F]fluorodeprenyl,[13] 6-[^{18}F]fluoro-*N*-methyl-*N*-(prop-2-yn-1-yl)-hexan-1-amine,[14] *N*-[(2*S*)-1-[^{18}F]fluoro-3-phenylpropan-2-yl]-*N*-methylprop-2-yn-1-amine,[15] [^{18}F]fluororasagiline.[16] A multistep radiosynthesis of DL-4-[^{18}F]fluorodeprenyl and undesired radiometabolites such as [^{18}F]fluoroamphetamine and [^{18}F]fluorometamphetamine from *N*[(2*S*)-1-[^{18}F]fluoro-3-phenylpropan-2-yl]-*N*-methyl-prop-2-yn-1-amine and radiometabolite [^{18}F]fluorohexanoic from 6-[^{18}F]fluoro-*N*-methyl-*N*-(prop-2-yn-1-yl)hexan-1-amine preclude their efficient routine use. In addition [^{18}F]fluoro rasagiline while binding with high affinity to MAO-B revealed a continuing increase in radioactivity over time hinting to undesired radiometabolite(s) that may complicate quantification.[16] Among all these irreversible MAO-B inhibitor PET radioligands [^{11}C]L-deprenyl is the one most widely used in both preclinical and clinical studies. However, the short half-life of carbon-11 (20.4 min) makes the tracers less suitable for distribution to PET centers not equipped with an on-site cyclotron. Therefore, there is a high interest in the development of a fluorine-18 labeled MAO-B inhibitor with a longer half-life (110 min) as molecular imaging biomarker for the detection of MAO-B activity in brain.

In this project we designed one heteroaromatic propargylamine derivative ((*S*)-*N*-(1-fluoro-3-(furan-2-yl)propan-2-yl)-*N*-methylprop-2-yn-1-amine (**5**)) and two aliphatic propargylamine derivatives ((*S*)-1-fluoro-*N*,4-dimethyl-*N*-(prop-2-ynyl)pent-4-en-2-amine (**10**) and (*S*)-1-fluoro-*N*,4-dimethyl-*N*-(prop-2-ynyl)pentan-2-amine (**15**)). Our aims were (i) to prepare the precursors and reference standards and to develop efficient synthetic methods for labeling these radioligands with fluorine-18 (ii) to evaluate their binding to MAO-B in various brain structures in post mortem human brain slices using an autoradiography technique and (iii) to evaluate the in vivo characteristics by PET measurement in a non-human primate.

2. Results and discussion

2.1. Chemistry

Three novel fluorinated derivatives of propargyl amine **5**, **10** and **15** (Scheme 1) were synthesized. Three appropriate chloro-precursors **4**, **9** and **14** were needed to be synthesized in order to label compounds **5**, **10** and **15** with fluorine-18 to obtain respective radioligands **16** and **18**.

Amines **2**, **7** and **12** were prepared from commercially available amino acid **1** ((*S*)-2-(*tert*-butoxycarbonylamino)-4-methylpent-4-enoic acid), **6** ((*S*)-*tert*-butyl 1-(furan-2-yl)-3-hydroxypropan-2-ylcarbamate) and amino acid **11** ((*S*)-4-methyl-2-(methylamino) pentanoic acid) by reduction with $LiAlH_4$ following a previously described procedure.[17] Amino alcohols **2**, **7** and **12** were alkylated with propargyl bromide[18] and the obtained alcohols **3**, **8** and **13**, respectively, were chlorinated upon treatment with mesyl chloride. A mixture of two chlorinated isomers **4A** and **4B** were formed from **3** and the mixture of **9A** and **9B** was formed from **8**. Compounds **14A** and **14B** were formed from **13**. The formation of chlorinated corresponding isomeric mixtures **4A** and **4B**, **9A** and **9B** and **14A** and **14B** can be explained by a corresponding intermediate aziridinium ion resulting from an intramolecular nucleophilic attack (S_Ni) of the free electron pair of the nitrogen.[15,19] Chlorides were then formed by subsequent nucleophilic attack (S_N2) of Cl^- at the corresponding reactive position of aziridinium ion **20** (Scheme 2).

Fluorides **5** and **10** were synthesized from amino alcohols **3** and **8** by fluorination with diethylamino sulfurtrifluoride (DAST) and fluoride **15** was synthesized from amino alcohol **13** by fluorination with triethylamine trihydrofluoride. In analogy to the chlorination described above, the fluorination gave rise to regioisomeric mixtures, which could be separated by column chromatography.

2.2. In vitro Inhibition of MAO-A and MAO-B

IC_{50} values for inhibition of MAO-B and MAO-A were determined based on the rate of the inhibition of kynuramine oxidation for compounds **5**, **10** and **15**. Compound **5** inhibited MAO-B with an IC_{50} of 664 nM while it was not inhibiting MAO-A (IC_{50} >2 μM). Compound **10** inhibited MAO-B with an IC_{50} of 208.5 ± 13.44 nM and did not inhibit MAO-A (IC_{50} >2 μM). Compound **15** featured an IC_{50} of 131.5 ± 0.71 nM for its MAO-B inhibitory activity while it was not inhibiting MAO-A (IC_{50} >2 μM). L-deprenyl was used as reference compound. It inhibited MAO-B with an IC_{50} of 56 ± 18.5 nM. Thus, compounds **10** and **15** inhibited MAO-B in a range comparable to that of the therapeutically used compound deprenyl, and were chosen to label with fluorine-18 for further investigation by ARG. Since compound **5** had the lowest affinity it was not considered for further evaluation.

2.3. Radiochemistry

The radiolabeling was achieved by one step nucleophilic substitution reactions of the chloride precursors (mixture of **9A**, **9B** and **14A**, **14B**) by [^{18}F]fluoride in presence of $K_{2.2.2}$ and K_2CO_3 as shown in Scheme 3. Azeotropic drying was performed before the dried $K[^{18}F]F^-K_{2.2.2}$ complex was treated with the adequate chloride precursor in anhydrous DMSO. The reaction mixtures were heated to form the respective fluorine-18 labeled product. Compound **16** was purified from the isomeric mixture of **16** and **17** as well as compound **18** was purified from the isomeric mixture of **18** and **19**

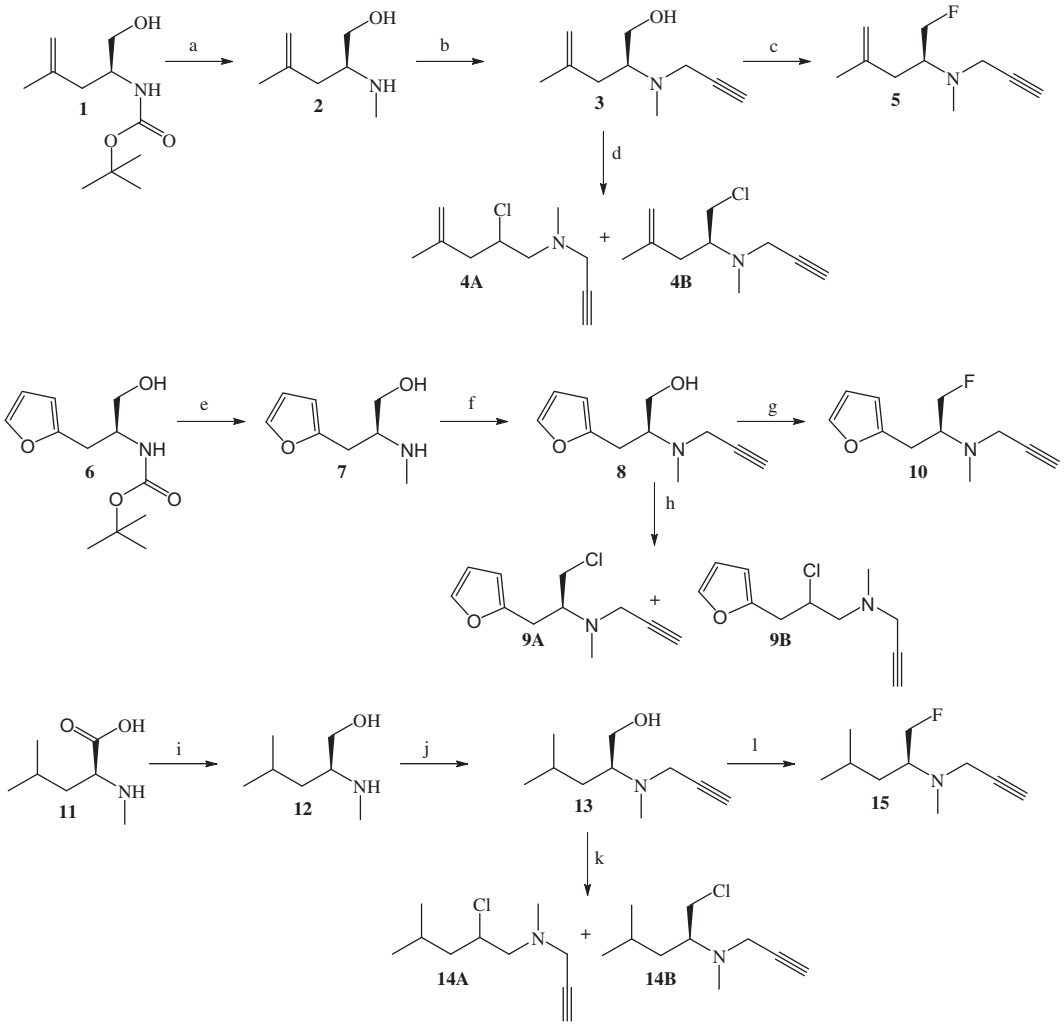

Scheme 1. Synthesis of precursors (**4A** + **4B**, **9A** + **9B** and **14A** + **14B**) and reference standards (**5**, **10** and **15**) for radiolabeling with fluorine-18. Conditions: (a) LAH; (b) K_2CO_3/propargyl bromide; (c) DAST; (d) pyridine/mesyl chloride; (e) LAH; (f) K_2CO_3/propargyl bromide; (g) DAST; (h) TEA/mesyl chloride; (i) LAH; (j) K_2CO_3/ propargyl bromide; (k) TEA/mesyl chloride; (l) TEA/DAST.

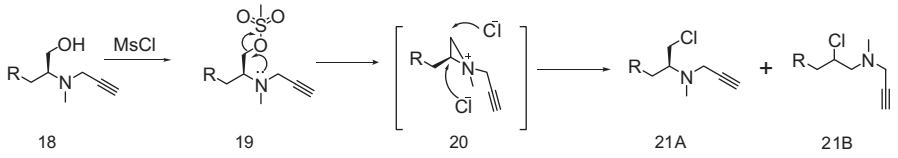

Scheme 2. Proposed mechanism for the formation of two chlorinated isomers **21A** and **21B**.

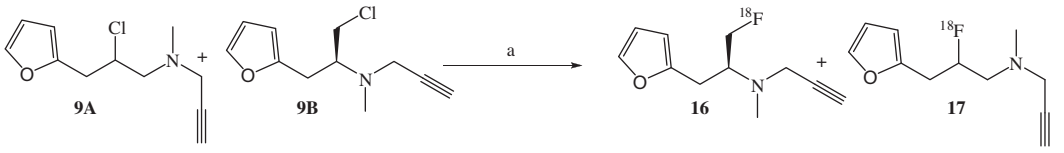

Scheme 3. Radiosynthesis of (*S*)-*N*-(1-[^{18}F]fluoro-3-(furan-2-yl)propan-2-yl)-*N*-methylprop-2-yn-1-amine (**16**). Conditions: a: K^{18}F, K-2,2,2/DMSO/K_2CO_3.

by semi preparative HPLC. The overall radiosynthesis including fluorination, HPLC purification, and evaporation of the solvent and radiotracer formulation was completed in a time range of 70–80 min (See Scheme 4).

The incorporation yield of the fluorination reactions from fluorine-18 ion varied from 40% to 60%, and the radiochemical purity was greater than 99% for both **16** and **18**. The specific radioactivity for **18** was >200 GBq/μmol. The identities of the labeled compounds were confirmed by co-injection of their corresponding fluorine-19 analogues **10** and **15** using analytical HPLC. Both radioligands were found to be stable in PBS buffered solution (pH = 7.4) for the duration of 150 min.

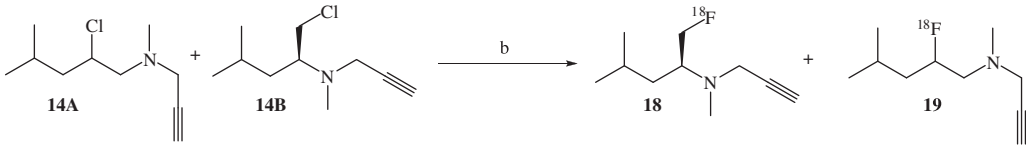

Scheme 4. Radiosynthesis of (*S*)-1-[^{18}F]fluoro-*N*,4-dimethyl-*N*-(prop-2-ynyl)pentan-2-amine (**18**). Conditions: b: K^{18}F, K-2,2,2/DMSO/K_2CO_3.

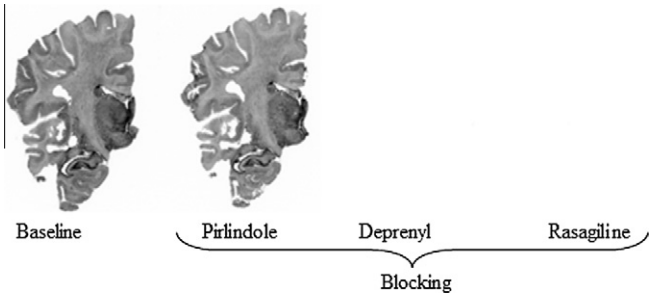

Figure 2. Autoradiograms of coronal slices of a human brain labeled with **18** at baseline condition and during incubation with pirlindole (10 μM), L-deprenyl (10 μM) and rasagiline (10 μM).

2.4. Autoradiography

Both novel MAO-B fluorine-18 labeled propargylamines **16** and **18** were tested in human whole hemisphere autoradiography experiments on postmortem brain tissue, obtained from deceased subjects with no sign of any brain disorders.

The total brain binding pattern, that is binding comprising specific and non-specific binding, with compound **16** displayed binding in the basal ganglia, thalamus, and cortex, with special regard to the hippocampus. For blocking, the MAO-B ligands L-deprenyl, rasagiline and the MAO-A ligand pirlindole, have been used in 10 μM concentrations. Using the MAO-B ligands L-deprenyl and rasagiline the binding of **16** was completely blocked, whereas the MAO-A ligand pirlindole also could partly block the total binding (Supplementary data). This indicated that **16** is not a selective radioligand for the MAO-B enzyme.

The total binding patterns of **18**, that is binding comprising specific and non-specific binding, are displayed in whole hemisphere brain slices obtained from control subjects. The signal intensities were highest in hippocampus, putamen, caudate nucleus and thalamus (Fig. 2). In order to test the specificity of the compound the binding was blocked with an excess (10 μM) of the MAO-B ligands L-deprenyl and rasagiline and of the MAO-A ligand pirlindole, respectively (Fig. 2). The MAO-B ligands rasagiline and L-deprenyl completely blocked the total binding of **18**, whereas the MAO-A ligand pirlindole did not block the total binding. These observations indicated that compound **18** is a selective radioligand of the MAO-B enzyme. Consequently, it was chosen for further examinations using PET measurements of its brain uptake and distribution in a cynomolgus monkey.

2.5. PET measurements in cynomolgus monkey

The uptake of the radioactive compound **18** in a cynomolgus monkey brain as a function of post injection time is shown in Figure 3. Compound **18** readily crosses the blood-brain barrier and binds rapidly to its target sites. The uptake was highest in the striatum and thalamus and lower in the cerebellum and cortical areas (Fig. 4B), consistent with the known distribution of in vivo MAO-B activity as previously reported for [^{11}C]deprenyl[10] and [^{18}F]fluorodeprenyl.[20] For [^{11}C]deprenyl and [^{18}F]fluorodeprenyl the uptake in striatum is higher than in thalamus whereas the inverse was observed for compound 18. The higher uptake in the thalamus relatively to the striatum could be explained either by lower in vivo selectivity of the radioligand for MAO-B or by possible blood-flow related distribution of radiometabolites entering the brain. The brain uptake in a baseline condition was high (250% SUV at 4 min) (Fig. 4A). Due to the irreversible binding kinetics, compound **18** did not show any wash-out from the brain.

2.6. Radiometabolite analysis

The recovery of radioactivity from plasma into acetonitrile after deproteinization was higher than 95%. HPLC analysis of plasma following injection of **18**, which eluted at 7.3 min, revealed the presence of five more major peaks, M1, M2, M3, M4 and M5 with retention times of 2.0, 3.4, 3.7, 4.2 and 6.2 min, respectively (Fig. 5A). The parent compound was less abundant at 45 min representing approximately 20% of the plasma radioactivity and it decreased to 12% at 120 min (Fig. 5B). The identity of the radiometabolites was not further analyzed. All the radiometabolites had shorter HPLC retention times than the unchanged radioligand indicating that they are less lipophilic than the parent compound. However, considering the retention time of the some of the radiometabolite peaks compared with the retention time of the parent radio peak, it could be possible that the increasing radioactivity

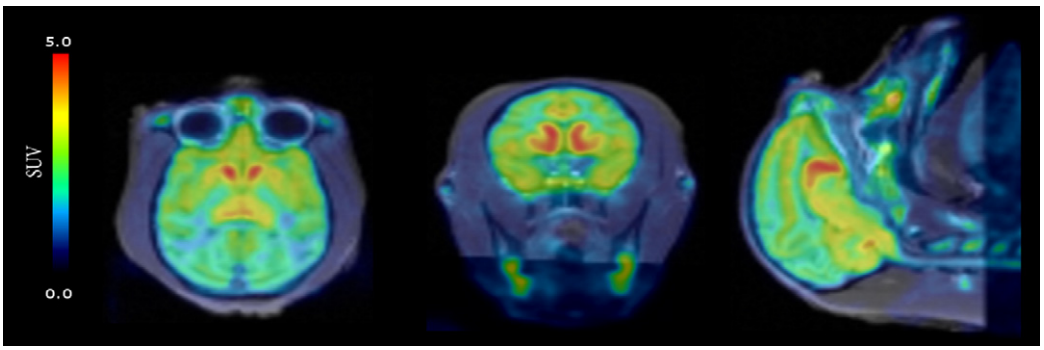

Figure 3. PET images of **18** co-registered with MRI and averaged between 9 and 120 min in the horizontal (left), coronal (middle) and sagittal (right) projections.

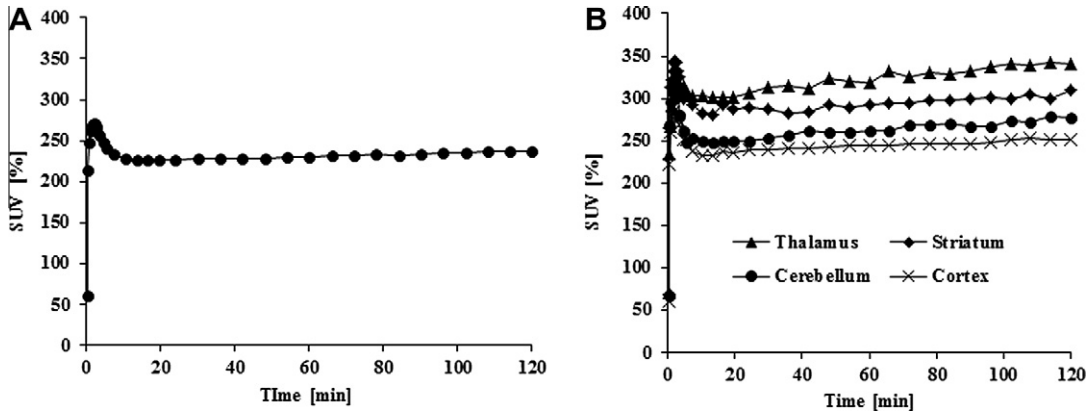

Figure 4. Brain uptake expressed as percent standardized uptake value (%SUV). (A) Time activity curves after iv injection of **18** in whole brain; (B) time activity curves of **18** in different brain regions.

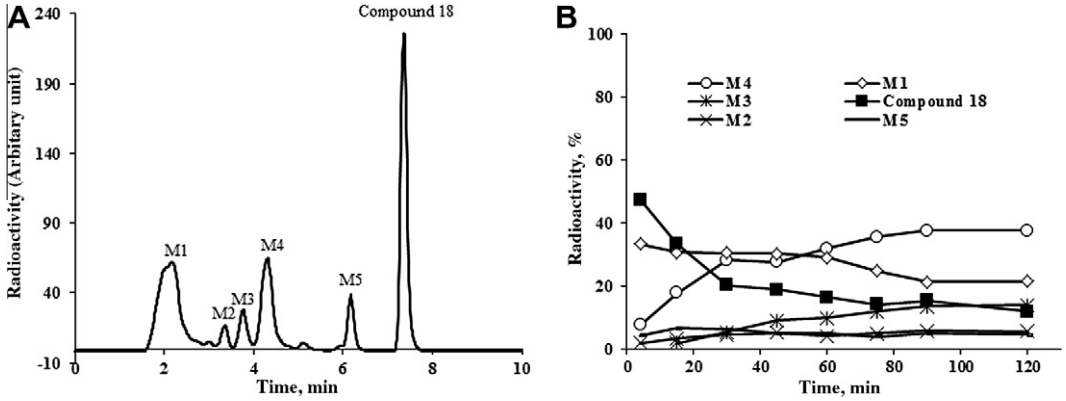

Figure 5. Metabolite analysis during the course of the PET measurements. A: A representative HPLC chromatogram 15 min after injection of **18** showing the retention times of the metabolites and the parent compound, B: The in vivo metabolism of **18** is shown as the relative plasma composition of radiometabolites and parent compound in% of total plasma radioactivity that was injected .

over time in the brain could be due to the radiometabolite(s) entering in to the brain.

3. Conclusion

The present study demonstrated that the radioligand (*S*)-1-[^{18}F]fluoro-*N*,4-dimethyl-*N*-(prop-2-ynyl)pentan-2-amine (**18**) was efficiently labeled with fluorine-18 and has nanomolar in vitro binding affinity to recombinant MAO-B (IC_{50} = 131 nM) and a more than 15 times lower affinity to MAO-A (IC_{50} >2 μM). In post-mortem human brain autoradiography compound **18** exhibited high specificity to regions with high MAO-B activity. Accordingly, PET measurement in a cynomolgus monkey showed a high brain uptake in known MAO-B rich regions. These results suggest that (*S*)-1-[^{18}F]fluoro-*N*,4-dimethyl-*N*-(prop-2-ynyl)pentan-2-amine (**18**) may be a potentially useful PET radiotracer for visualization of MAO-B activity in human brain.

4. Materials and methods

4.1. Chemistry

NMR spectra were recorded on Varian Unity-400 and Bruker Avance 400 (^{1}H, 400 MHz and ^{13}C, 100 MHz), and Bruker Avance 600 III (^{1}H, 600 MHz) NMR instruments. ^{1}H NMR spectra were referenced internally on $CDCl_3$ (δ 1H 7.26) and ^{13}C NMR spectra were referenced internally on $CDCl_3$ (δ 13C 77.20). For the purification of (*S*)-*N*-(1-[^{18}F]fluoro-3-(furan-2-yl)propan-2-yl)-*N*-methylprop-2-yn-1-amine and (*S*)-1-[^{18}F]fluoro-*N*,4-dimethyl-*N*-(prop-2-ynyl)pentan-2-amine high performance liquid chromatographic (HPLC) analysis was performed with a Merck–Hitachi gradient pump and a Merck–Hitachi, L-4000 variable wavelength UV-detector. A ACE 5 C-18 HL HPLC column (250 × 10 mm, 5 μm, Advanced Chromatography) was used with a mobile phase CH_3CN/10 mM H_3PO_4 (10/90) and flow rate of 3 mL/min. Specific radioactivity (SA), quality control and plasma analysis were determined by analytical HPLC using a μ-Bondapak reverse phase HPLC column (C18, 3.9 mm × 300 mm, 10 μm, Waters) with mobile phase CH_3CN/10 mM H_3PO_4 (15/85) and flow rate of 2 mL/min. LC–MS was performed using a Waters Quattra-Tof Premier micro mass spectrometer, or Waters SQD 3001 single quadrupole mass spectrometer, coupled to Waters Acquity UPLC instruments. Analytical TLC was carried out on 0.25 mm silica gel plates. All solvents and chemicals were obtained from commercial sources and used without further purification.

4.2. Synthesis of (*S*)-4-methyl-2-(methylamino)pent-4-en-1-ol (2)

To a solution of (*S*)-*tert*-butyl 1-hydroxy-4-methylpent-4-en-2-ylcarbamate dicyclohexyl amine salt (**1**, 5.0 g, 12.2 mmol) in dry THF (15 mL) was added lithium aluminium hydride (LAH) (21.7 mmol, 1 M solution in THF) dropwise at −5 °C. The reaction mixture was refluxed for overnight and cooled to −5 °C. Unreacted

LAH was quenched with aq NaOH (0.8 g, 20 mmol, 2 N) and the mixture was stirred at room temperature for additional 30 min. The mixture was filtered, and was washed with diethyl ether (100 mL). The filtrate was dried over $MgSO_4$ and solvent was removed under reduced pressure to obtain the product as colorless oil. The final product was obtained as dicyclohexyl amine salt (2.4 g, 7.7 mmol, 61.3%). The product was analyzed by NMR and LC–MS and used in the next step without further purification.

^{1}H NMR (400 MHz, $CDCl_3$) δ ppm 1.68–1.73 (m, 3H) 1.73–1.76 (m, 4H) 1.82–1.89 (m, 4H) 2.24 (t, J = 2.40 Hz, 1H) 2.35 (s, 4H) 2.40 (dd, J = 13.64, 4.04 Hz, 1H) 2.55 (tt, J = 10.61, 3.79 Hz, 1H) 3.02 (tt, J = 9.76, 4.52 Hz, 2H) 3.30 (dd, J = 10.86, 9.60 Hz, 1H) 3.41 (dd, J = 7.45, 2.40 Hz, 2H) 3.52 (dd, J = 10.86, 4.55 Hz, 1H) 4.72 (s, 1H) 4.77 (s, 1H).

^{13}C NMR (101 MHz, $CDCl_3$) δ ppm 25.36, 26.21, 34.28, 40.38, 53.10, 57.88, 62.43, 68.02, 76.76, 77.07, 77.39, 113.15 and 142.63.

LC–MS (+): m/z = 130.2 [(M+H)+].

4.3. Synthesis of (*S*)-4-methyl-2-(methyl(prop-2-ynyl)amino)-pent-4-en-1-ol (3)

To a solution of (*S*)-4-methyl-2-(methylamino)pent-4-en-1-ol dicyclohexyl amine salt (**2**, 2.4 g, 7.3 mmol) in dry THF (15 mL) was added potassium carbonate (4.0 g, 29.0 mmol) and stirred at room temperature 30 min. To the stirred solution propargyl bromide (2.3 g, 19.3 mmol) was added dropwise and the reaction mixture was stirred at room temperature for overnight, diluted with water (50 mL) and extracted with CH_2Cl_2 (3 × 50 mL). The organic phase was separated and washed with saturated $NaHCO_3$ solution (100 ml) and brine (100 ml). The organic layer was dried over $MgSO_4$ and filtered. The solvent was removed under reduced pressure to obtain the crude product. The crude product was purified by silica-gel column chromatography (EtOAc/hexane 30:70) and the final product (0.9 g, 5.4 mmol, 69.6%) resulted as light yellow oil. The product was analyzed by NMR, HPLC and LC–MS.

^{1}H NMR (400 MHz, $CDCl_3$) δ ppm 1.74 (s, 3H) 1.88 (d, J = 3.28 Hz, 1H) 2.35 (s, 3H) 2.40 (dd, J = 13.64, 4.04 Hz, 1H) 2.55 (tt, J = 10.61, 3.79 Hz, 1H) 2.98–3.06 (m, 1H) 3.30 (dd, J = 10.86, 9.60 Hz, 1H) 3.35–3.47 (m, 2H) 3.52 (dd, J = 10.86, 4.55 Hz, 1H) 4.69–4.74 (m, 1H) 4.74–4.80 (m, 1H).

^{13}C NMR (101 MHz, $CDCl_3$) δ ppm 25.36, 26.23, 28.39, 34.31, 35.61, 43.41, 53.10, 60.79, 61.03, 113.01 and 142.61.

LC–MS (+): m/z = 168.2 [(M+H)+].

4.4. Synthesis of 2-chloro-*N*,4-dimethyl-*N*-(prop-2-ynyl)pent-4-en-1-amine (4A) and (*S*)-1-chloro-*N*,4-dimethyl-*N*-(prop-2-ynyl)pent-4-en-2-amine (4B)

A mixture of **3** (260 mg, 1.55 mmol) and pyridine (500 µl, 6.21 mmol) in CH_2Cl_2 (3.5 ml) was stirred at room temperature for 30 min. To the stirred mixture mesyl chloride (356 mg, 240 µl, 3.11 mmol) was added dropwise at −5 °C and the reaction mixture was stirred at room temperature for additional 30 min. Saturated aqueous Na_2CO_3 solution (1 mL) was added to the reaction mixture and stirred for further 30 min. The organic layer was partitioned between CH_2Cl_2 (45 ml) and water (30 ml). The organic phase was separated and washed with saturated $NaHCO_3$ solution (10 ml) and brine (10 ml), dried over $MgSO_4$ and filtered. The solvent was removed under reduced pressure to obtain the crude product as light yellow oil. The crude product was purified by silica-gel column chromatography (hexane/ether 3:1) and final product (250.0 mg, 87%, 1.35 mmol) was obtained as light yellow oil. The product was analyzed by NMR, HPLC and LC–MS. The final product was a mixture of **4A** (major) and **4B** (minor).

Mixture of isomers: ^{1}H NMR (400 MHz, $CDCl_3$) δ ppm 2.38 (4B, s, 3H) 2.44 (4A, s, 3H) 2.61 (dd, J = 14.78, 4.93 Hz, 1H) 2.72 (dd, J = 6.69, 2.40 Hz, 2H) 3.07 (dq, J = 8.34, 5.31 Hz, 1H) 3.48 (4A, d, J = 7.07 Hz, 2H) 3.52 (4A, dd, J = 7.83, 2.53 Hz, 2H) 3.61 (4B, dd, J = 11.62, 4.80 Hz, 1H) 3.69 (4Bdd, J = 11.62, 4.80 Hz, 1H) 4.08 (4B, dddd, J = 8.75, 7.42, 5.94, 5.18 Hz, 1H) 4.80–4.86 (4A + 4B m, 4H).

^{13}C NMR (101 MHz, $CDCl_3$) δ ppm 34.18, 37.39, 37.66, 42.20, 43.24, 44.75, 45.97, 57.56, 60.69, 62.08, 113.59 and 143.04.

LC–MS (+): m/z = 187.0 [(M+H)+].

4.5. Synthesis of (*S*)-1-fluoro-*N*,4-dimethyl-*N*-(prop-2-ynyl)-pent-4-en-2-amine (5)

To the stirred solution of **3** (115 mg, 0.69 mmol) in tetrahydrofuran (3 mL) diethylamino sulfurtrifluoride (166.20 µl, 1.03 mmol) was added dropwise at −5 °C and the reaction mixture was stirred for additional 10 min at the same temperature. Saturated sodium carbonate (2.0 mL) was added to the reaction mixture in order to quench the unreacted diethylamino sulfurtrifluoride. The organic layer was partitioned between CH_2Cl_2 (15 ml) and water (10 ml). The organic phase was separated and washed with brine (10 ml) and dried over $MgSO_4$ and filtered. The solvent was removed under reduced pressure to obtain the crude product as yellow oil. Due to the high volatility of the compound the crude product was purified by silica-gel column chromatography using pentane/ether (3:1) and gave the final product (90 mg, 0.53 mmol, 77.3%). The product was analyzed by NMR, HPLC and LC–MS.

^{1}H NMR (400 MHz, $CDCl_3$) δ ppm 2.41 (s, 3H) 2.49 (s, 3H) 2.68–2.76 (m, 3H) 3.11 (dq, 1H) 3.46–3.55 (m, 4H) 3.66 (dd, 1H) 3.64 (dd, 1H) 4.12 (m, 1H) 4.82–4.89 (m, 3H).

^{13}C NMR (101 MHz, $CDCl_3$) δ ppm 34.21, 37.36, 37.68, 42.28, 43.31, 44.74, 46.00, 57.60, 60.68, 62.11, 113.64 and 143.14.

LC–MS (+): m/z = 170.3 [(M+H)+].

4.6. Synthesis of (*S*)-3-(furan-2-yl)-2-(methylamino)propan-1-ol (7)

To a solution of (*S*)-*tert*-butyl 1-(furan-2-yl)-3-hydroxypropan-2-ylcarbamate dicyclohexyl amine salt (**6**, 3.8 g, 8.7 mmol) in dry THF (15 mL) was added lithium aluminium hydride (LAH) (21.7 mmol, 1 M solution in THF) dropwise at −5 °C. The reaction mixture was refluxed for overnight and cooled to −5 °C. Unreacted LAH was quenched with aq NaOH (0.6 g, 15.0 mmol, 2 N) and the mixture was stirred at room temperature for additional 30 min. The mixture was filtered, and was washed with diethyl ether (100 mL). The filtrate was dried over $MgSO_4$ and solvent was removed under reduced pressure to obtain the product as colorless oil (2.4 g, 7.13 mmol, 81.9%). The product was analyzed by NMR and LC–MS and used in the next step without further purification.

^{1}H NMR (300 MHz, $CDCl_3$) δ ppm 2.41 (s, 3H) 2.51–2.57 (m, 2H), 2.76–2.86 (m, 3H) 3.34 (dd, 1H) 3.61–3.66 (m, 2H), 6.06 (dd, 1H) 6.29 (dd, 1H) 7.32 (d, 1H).

^{13}C NMR (101 MHz, $CDCl_3$) δ ppm 25.36, 34.31, 53.04, 59.69, 62.43, 106.98, 110.33, 141.58 and 152.

LC–MS (+): m/z = 156.3 [(M+H)+].

4.7. Synthesis of (*S*)-3-(furan-2-yl)-2-(methyl(prop-2-ynyl)-amino)propan-1-ol (8)

To a solution of (*S*)-3-(furan-2-yl)-2-(methylamino)propan-1-ol dicyclohexyl amine salt (7, 1.55 g, 4.6 mmol) in dry THF (10 mL) was added potassium carbonate (2.0 g, 14.5 mmol) and stirred at room temperature 30 min. To the stirred solution propargyl bromide (1.65 g, 9.65 mmol) was added dropwise and the reaction mixture was stirred at room temperature for overnight, diluted with water (30 mL) and extracted with CH_2Cl_2 (3 × 30 mL). The organic phase was separated and washed with saturated $NaHCO_3$

solution (100 ml) and brine (100 ml). The organic layer was dried over $MgSO_4$ and filtered. The solvent was removed under reduced pressure to obtain the crude product. The crude product was purified by silica-gel column chromatography (EtOAc/hexane 30:70) and the final product (850 mg, 4.4 mmol, 95.6%) resulted as light yellow oil. The product was analyzed by NMR, HPLC and LC–MS.

^{1}H NMR (300 MHz, $CDCl_3$) δ ppm 2.25 (t, J = 2.45 Hz, 1H) 2.38 (s, 3H) 2.50 (dd, J = 14.88, 9.04 Hz, 1H) 3.02 (dd, J = 14.88, 4.90 Hz, 1H) 3.18 (tt, J = 9.23, 4.71 Hz, 1H) 3.32–3.41 (m, 3H) 3.43–3.52 (m, 1H) 6.02 (dd, J = 3.11, 0.66 Hz, 1H) 6.27 (dd, J = 3.01, 1.88 Hz, 1H) 7.30 (d, J = 0.75 Hz, 1H).

^{13}C NMR (101 MHz, $CDCl_3$) δ ppm 24.81, 35.59, 43.56, 61.00, 62.81, 72.88, 80.35, 106.59, 110.43, 141.32 and 152.73.

LC–MS (+): m/z = 194.2 [(M+H)+].

4.8. Synthesis of *N*-(2-chloro-3-(furan-2-yl)propyl)-*N*-methylprop-2-yn-1-amine (9A) and (*S*)-*N*-(1-chloro-3-(furan-2-yl)propan-2-yl)-*N*-methylprop-2-yn-1-amine (9B)

A mixture of **8** (450 mg, 2.33 mmol) and pyridine (750 µl, 9.31 mmol) in CH_2Cl_2 (6.0 ml) was stirred at room temperature for 30 min. To the stirred mixture mesyl chloride (400 mg, 270 µl, 3.5 mmol) was added dropwise at −5 °C and the reaction mixture was stirred at room temperature for additional 30 min. Saturated aqueous Na_2CO_3 solution (2 mL) was added and stirred for further 30 min. The organic layer was partitioned between CH_2Cl_2 (90 ml) and water (50 ml). The organic phase was separated and washed with saturated $NaHCO_3$ solution (30 ml) and brine (30 ml), dried over $MgSO_4$ and filtered. The solvent was removed under reduced pressure to obtain the crude product as light yellow oil. The crude product was purified by silica-gel column chromatography (hexane/ether 3:1) and final product (342 mg, 69.3%, 1.61 mmol) was obtained as light yellow oil. The product was analyzed by NMR, HPLC and LC–MS. The final product was a mixture of **9A** (major) and **9B** (minor). ^{1}H NMR reflects only the major isomer **9A**.

^{1}H NMR (400 MHz, $CDCl_3$) δ ppm 2.26 (t, J = 2.40 Hz, 1H) 2.48 (s, 3H) 3.53 (t, J = 2.78 Hz, 2H) 3.56–3.68 (m, 2H) 6.10–6.20 (m, 1H) 6.30 (dd, J = 3.03, 2.02 Hz, 1H) 7.30–7.36 (m, 1H).

^{13}C NMR (101 MHz, $CDCl_3$) δ ppm 14.13, 22.70, 27.71, 31.64, 34.98, 37.92, 42.14, 43.55, 44.63, 46.05, 62.00, 73.33, 107.12, 110.40, 141.44 and 152.58

LC–MS (+): m/z = 212.1 [(M+H)+].

4.9. Synthesis of (*S*)-*N*-(1-fluoro-3-(furan-2-yl)propan-2-yl)-*N*-methylprop-2-yn-1-amine (10)

A mixture of **8** (400 mg, 2.07 mmol) in tetrahydrofuran (3 mL) diethylamino sulfurtrifluoride (166.20 µl, 1.03 mmol) was added dropwise at -5 °C and the reaction mixture was stirred for additional 10 min at the same temperature. Saturated sodium carbonate (2.0 mL) was added to quench the unreacted diethylamino sulfurtrifluoride. The organic layer was partitioned between CH_2Cl_2 (15 ml) and water (10 ml). The organic phase was separated and washed with brine (10 ml) and dried over $MgSO_4$ and filtered. The solvent was removed under reduced pressure to obtain the crude product as yellow oil. Due to the high volatility of the compound the crude product was purified by silica-gel column chromatography using pentene/ether (3:1) and gave the final product (150 mg, 0.77 mmol, 37%). The product was analyzed by NMR, HPLC and LC–MS.

^{1}H NMR (400 MHz, $CDCl_3$) δ ppm 2.26 (t, J = 2.40 Hz, 1H) 2.48 (s, 3H) 2.85 (dd, J = 15.03, 9.22 Hz, 1H) 2.94–3.03 (m, 1H) 3.16–3.31 (m, 1H) 3.48 (d, J = 2.27 Hz, 2H) 4.37–4.46 (m, 1H) 4.46–4.58 (m, 1H) 4.58–4.66 (m, 1H) 6.10 (d, J = 3.28 Hz, 1H) 6.28–6.33 (m, 1H) 7.32 (s, 1H).

^{13}C NMR (101 MHz, $CDCl_3$) δ ppm 37.96, 43.93, 61.07, 61.25, 72.83, 80.16, 82.31, 84.01, 106.89, 110.41, 141.37 and 152.74.

LC–MS (+): m/z = 196.1 [(M+H)+].

4.10. Synthesis of (*S*)-4-methyl-2-(methylamino)pentan-1-ol (12)

To a solution of (*S*)-4-methyl-2-(methylamino)pentanoic acid hydrochloride salt (**11**, 5.0 g, 27.5 mmol) in dry THF (20 mL) was added lithium aluminium hydride (LAH) (33.0 mmol, 1 M solution in THF) dropwise at −5 °C. The reaction mixture was refluxed for overnight and cooled to -5 °C. Unreacted LAH was quenched with aq NaOH (0.8 g, 20.0 mmol, 2 N) and the mixture was stirred at room temperature for additional 30 min. The mixture was filtered, and was washed with diethyl ether (100 mL). The filtrate was dried over $MgSO_4$ and solvent was removed under reduced pressure to obtain the product as colorless oil (3.5 g, 26.2 mmol, 97.0%). The product was analyzed by NMR and LC–MS and used in the next step without further purification.

^{1}H NMR (400 MHz, $CDCl_3$) δ ppm 0.87 (d, J = 6.57 Hz, 6H) 1.15 (dt, J = 13.77, 7.01 Hz, 1H) 1.29 (ddd, J = 13.71, 7.52, 6.32 Hz, 1H) 1.59 (spt, J = 6.57 Hz, 1H) 2.36 (s, 3H) 2.51 (qd, J = 6.57, 3.79 Hz, 2H) 3.24 (dd, J = 10.86, 6.32 Hz, 1H) 3.58 (dd, J = 10.61, 3.79 Hz, 1H) 3.66–3.74 (m, 1H).

^{13}C NMR (101 MHz, $CDCl_3$) δ ppm 22.71, 23.10, 24.98, 25.61, 33.37, 40.47, 58.50, 62.82 and 67.96.

LC–MS (+): m/z = 132.1 [(M+H)+].

4.11. Synthesis of (*S*)-4-methyl-2-(methyl(prop-2-ynyl)amino)-pentan-1-ol (13)

To a solution of (*S*)-4-methyl-2-(methylamino)pentan-1-ol (**11**, 3.6 g, 27.4 mmol) in dry THF (18 mL) was added potassium carbonate (8.0 g, 58.0 mmol) and stirred at room temperature 30 min. To the stirred solution propargyl bromide (4.9 g, 41.1 mmol) was added dropwise and the reaction mixture was stirred at room temperature for overnight, diluted with water (50 mL) and extracted with CH_2Cl_2 (3 × 50 mL). The organic phase was separated and washed with saturated $NaHCO_3$ solution (100 ml) and brine (100 ml). The organic layer was dried over $MgSO_4$ and filtered. The solvent was removed under reduced pressure to obtain the crude product. The crude product was purified by silica-gel column chromatography (diethyl ether/pentane 25:75) and the final product (3.0 g, 17.7 mmol, 64.6%) resulted as light yellow oil. The product was analyzed by NMR, HPLC and LC–MS.

^{1}H NMR (400 MHz, $CDCl_3$) δ ppm 0.90 (t, J = 6.19 Hz, 6H) 1.03 (ddd, J = 13.71, 9.16, 4.93 Hz, 1H) 1.36–1.44 (m, 1H) 1.46–1.59 (m, 1H) 2.23 (t, J = 2.40 Hz, 1H) 2.31 (s, 3H) 2.83–2.92 (m, 1H) 3.06 (br. s., 1H) 3.24–3.43 (m, 3H) 3.52 (dd, J = 10.86, 4.80 Hz, 1H).

^{13}C NMR (101 MHz, $CDCl_3$) δ ppm 22.08, 23.75, 25.48, 34.28, 35.72, 43.20, 61.23, 72.52, 76.75, 77.07, 77.38 and 80.66.

LC–MS (+): m/z = 170.1 [(M+H)+].

4.12. Synthesis of 2-chloro-*N*,4-dimethyl-*N*-(prop-2-ynyl)-pentan-1-amine (14A) and (*S*)-1-chloro-*N*,4-dimethyl-*N*-(prop-2-ynyl)pentan-2-amine (14B)

A mixture of **13** (625 mg, 3.69 mmol) and triethylamine (1.5 mg, 14.8 mmol) in CH_2Cl_2 (7.0 ml) was stirred at room temperature for 30 min. To the stirred mixture mesyl chloride (846 mg, 5712 µl, 7.38 mmol) was added dropwise at −5 °C and the reaction mixture was stirred at room temperature for additional 30 min. Saturated aqueous Na_2CO_3 solution (3 mL) was added to the reaction mixture. The mixture wasstirred for further 30 min. The organic layer was partitioned between CH_2Cl_2 (150 ml) and water (30 ml). The organic phase was separated and washed with

saturated $NaHCO_3$ solution (50 ml) and brine (50 ml), dried over $MgSO_4$ and filtered. The solvent was removed under reduced pressure to obtain the crude product as light yellow oil. The crude product was purified by silica-gel column chromatography (pentane/ether 3:1) and final product (550 mg, 79%, 2.9 mmol) was obtained as light yellow oil. The product was analyzed by NMR, HPLC and LC–MS. The final product was a mixture of **14A** (major) and **14B** (minor).

^{1}H NMR (400 MHz, $CDCl_3$) δ ppm 0.91 (d, J = 6.57 Hz, 3H) 0.95 (d, J = 6.82 Hz, 3H) 1.54–1.66 (m, 2H) 1.95 (m, J = 13.71, 6.74, 6.74, 6.74, 6.74 Hz, 1H) 2.24 (t, J = 2.40 Hz, 1H) 2.37 (s, 3H) 2.64–2.75 (m, 2H) 3.39–3.51 (m, 2H) 3.94–4.04 (m, 1H).

^{13}C NMR (101 MHz, $CDCl_3$) δ ppm 21.20, 23.27, 25.15, 30.37, 42.15, 45.40, 45.98, 58.56, 62.76, 73.55, 76.74, 77.06 and 77.38.

LC–MS (+): m/z = 188,2 [(M+H)+].

4.13. Synthesis of (*S*)-1-fluoro-*N*,4-dimethyl-*N*-(prop-2-ynyl)-pentan-2-amine (15)

A mixture of **13** (205 mg, 1.21 mmol) and triethylamine (735.3 mg, 7.26 mmol) in CH_2Cl_2 (3 mL) diethylamino sulfurtrifluoride (166.20 μl, 1.03 mmol) was stirred at room temperature for 30 min. To the stirred solution triethylamine trihydrofluoride (667.7 mg, 4.14 mmol) was added drop wise and the mixture was at the same temperature for 10 min. To the stirred solution 1,1,2,2,3,3,4,4,4-nonafluorobutane-1-sulfonyl fluoride (1.25 g, 4.14 mmol) was added and the reaction mixture wad stirred at the room temperature for additional 60 min. The organic layer was partitioned between CH_2Cl_2 (60 ml) and water (30 ml). The organic phase was separated and washed with brine (10 ml) and dried over $MgSO_4$ and filtered. The solvent was removed under reduced pressure to obtain the crude product as yellow oil. Due to the high volatility of the compound the crude product was purified by silica-gel column chromatography using pentane/diethylether (gradient: 0–50%) and gave the final product (120 mg, 0.71 mmol, 58.6%). The product was analyzed by NMR, HPLC and LC–MS.

^{1}H NMR (400 MHz, $CDCl_3$) δ ppm 0.92–0.94 (m, 6H) 1.70 (dq, J = 13.52, 6.78 Hz, 1H) 1.85 (dt, J = 6.76, 3.32 Hz, 1H) 2.20–2.24 (m, 1H) 2.41 (s, 3H) 2.92–3.06 (m, 1H) 3.43 (d, J = 2.27 Hz, 2H) 3.72–3.77 (m, 1H) 4.45 (dd, J = 4.67, 2.15 Hz, 1H) 4.57 (dd, J = 4.67, 2.15 Hz, 1H).

^{13}C NMR (101 MHz, $CDCl_3$) δ ppm 22.05, 23.26, 24.56, 42.24, 42.51, 46.36, 60.00, 73.26, 78.44, 90.37 and 92.05.

LC–MS (ESI): m/z = 172.1 (M+1).

4.14. Radiochemistry

Fluorine-18 fluoride ($[^{18}F]F^-$) was produced from a GEMS PET trace Cyclotron using 16.4 MeV protons via the $^{18}O(p,n)$ ^{18}F reaction on ^{18}O enriched water ($[^{18}O]H_2O$) and $[^{18}F]F^-$ was isolated from $[^{18}O]H_2O$ on a preconditioned SepPak QMA light anion exchange cartridge and subsequently eluted from the cartridge with a solution of K_2CO_3 (1.8 mg, 13 μmol), Kryptofix 2.2.2 (4,7,13,16,21,24-hexaoxa-1,10-diazabicyclo- [8.8.8]hexacosane-$K_{2.2.2}$) (9.8 mg, 26 μmol) in water (85 μL, 18 MΩ) and MeCN (2 mL) to a reaction vessel (10 mL). The solvents were evaporated at 160 °C for 10–15 min under continuous nitrogen flow (70 mL/min) to form a dry complex of $[^{18}F]F^-/K_2CO_3$/K2.2.2 and the residue was cooled to room temperature (RT).

4.15. Synthesis of (*S*)-*N*-(1-[^{18}F]fluoro-3-(furan-2-yl)propan-2-yl)-*N*-methylprop-2-yn-1-amine (16) and *N*-(2-[^{18}F]fluoro -3-(furan-2-yl)propyl)-*N*-methylprop-2-yn-1-amine (17)

The precursor (**9A** and **B**) (~0.02 mmol, ~4 mg) in DMSO (500 μL) was added to the dry complex of $[^{18}F]$ F^-/K_2CO_3/K2.2.2. The closed reaction vessel was heated at 140 °C for 10 min. The reaction mixture was cooled to the room temperature and was diluted with water to a total volume of 2 mL before injecting to the HPLC for purification. The fluorine-18 labeled radioligand was purified by reverse phase HPLC on a μ-Bondapak C-18 column (300 × 7.8 mm, 10 μm; waters instruments) and MeCN–H_3PO_4 (0.01 M) (15:85 v/v) was used as the eluting solvent at a flow rate of 3 mL/min. Elute was monitored by a UV absorbance detector (λ = 214 nm) in series with a GM tube radioactivity detector. The isomeric mixture of **16** and **17** was separated by semi preparative high performance liquid chromatography (HPLC) ($t_{R(16)}$ = 12–14 min, $t_{R(17)}$ = 16–17 min) and the purification was performed in reverse-phase μ-Bondapak C-18 HPLC column (7.8 × 300 mm, 10 μm; Waters) with mobile phase [(MeCN/TFA (0.1%), 15:85 v/v]. The flow rate of the eluate was 4 mL/min through an absorbance detector (λ = 234 nm) coupled with a GM tube for radiation detection.The fraction of the desired compound (**16**) was collected and evaporated to dryness. The residue was dissolved in sterile disodiumphosphate phosphate buffered saline (PBS; pH = 7.4; 10 mL) and filtered through a sterile filter (0.22 μm; Millipore, Bedford, MA), yielding a sterile and pyrogen-free (<1.25 EU) solution of the radioligand.

4.16. Synthesis of (*S*)-1-[^{18}F]fluoro-*N*,4-dimethyl-*N*-(prop-2-ynyl)pentan-2-amine (18) and 2-[^{18}F]fluoro-*N*,4-dimethyl-*N*-(prop-2-ynyl)pentan-1-amine (19)

The precursor (**14A** and **14B**) (~0.018 mmol, ~3 mg) in DMSO (500 μL) was added to the dry complex of $[^{18}F]$ F^-/K_2CO_3/K2.2.2. The closed reaction vessel was heated at 130 °C for 15 min. The reaction mixture was cooled to the room temperature and was diluted with water to a total volume of 2 mL before injecting to the HPLC for purification. The fluorine-18 labeled radioligand was purified by reverse phase HPLC on a ACE 5 C18 C-18 column (250 × 10 mm, 5 μm waters instruments) and MeCN–H_3PO_4 (0.01 M) (10:90 v/v) was used as the eluting solvent at a flow rate of 3 mL/min. The isomeric mixture of **18** (t_R = 12–14 min) and **19** (t_R = 17–18 min) was separated by HPLC and the precursor was eluted at t_R = 19 min. A radioactive fraction corresponding the pure (*S*)-1-[^{18}F]fluoro-*N*,4-dimethyl-*N*-(prop-2-ynyl)pentan-2-amine (**18**) was collected and diluted with water (50 mL, 18 MΩ). The resulting mixture was loaded on to a pre-conditioned SepPak tC18 plus cartridge. The cartridge was washed with water (10 mL) and the isolated product, (S)-1-[^{18}F]fluoro-*N*,4-dimethyl-*N*-(prop-2-ynyl)pentan-2-amine (18) was eluted with 1 mL of ethanol in to a sterile vial containing phosphate buffer saline solution (PBS, 9 mL) and filtered through a sterile filter (0.22 μm; Millipore, Bedford, MA), yielding a sterile and pyrogen-free (<1.25 EU) solution of the radioligand.

4.17. Quality control and specific radioactivity (SA) determination

The radiochemical purity, identity and stability of **16** and **18** was determined by analytical HPLC using mobile phase CH_3CN/10 mM H_3PO_4 (15/85) and flow rate of 2 mL/min. The effluent was monitored with an UV absorbance detector (λ = 214 nm) coupled to a radioactive detector (β-flow, Beckman, Fullerton, CA). The identity of **16** and **18** was confirmed by co-injection with the authentic non-radioactive reference standards.

The SA of the product was measured by analytical HPLC using mobile phase CH_3CN/50 mM H_3PO_4 (15/85) at flow rate of 2 ml/min. SA was calibrated for UV absorbance (λ = 214 nm) response per mass of ligand and calculated as the radioactivity of the radioligand (GBq) divided by the amount of the associated carrier substance (μmol). Each sample was analyzed 3 times and compared to a reference standard also analyzed 3 times.

4.18. MAO inhibition determination

Human recombinant MAO-B and MAO-A enzymes prepared from insect cells were purchased from Sigma. The assays were designed to determine the inhibition of kynuramine oxidation in the presence of the compounds of interest according to Weissbach et al.[21] A calibration curve of kynuramine hydrobromide (Sigma) was determined at 360 nm and used for calculation of the enzyme activity (pmol/min) at the respective compound concentration. This relation was plotted and the IC_{50} determined using the software GraFit 5 (Version 5.0.6). The assays were performed as follows. The compounds were diluted 1:2 in each step in 50 mM phosphate buffered saline (pH 7.4) so that a concentration curve between 0.49 nM and 1000 nM was generated to determine the IC_{50} for MAO-B and between 0.98 and 2000 nM for determination of inhibition of MAO-A, respectively. Kynuramine hydrobromide at a concentration of 125 μM for MAO-B and 100 μM for MAO-A, respectively, and 2.5 U/ml enzyme were added and the reaction followed measuring the absorption at 360 nm in a 5 min interval over 30 min at 37 °C. The 30 min time point was used to determine IC_{50} values. As internal standards for MAO-B, pargyline and L-deprenyl and for MAO-A clorgyline were used.

4.19. In vitro autoradiography

Human brains without pathology were obtained from the Department of Forensic and Insurance Medicine, Semmelweis University, Budapest. The brains had been removed during forensic autopsy (control brains) and were handled in a manner similar to that described previously.[22–24] In the present experiment the post mortem time was 11 h until which the cadaver was stored at ±0 °C. After the removal of the brain it was kept at −85 °C until sectioning after which the whole hemisphere brain slices were kept at −25 °C until the autoradiographic procedures. Ethical permissions were obtained from the relevant Research Ethics Committee of the respective institutions. The sectioning of the brains and the autoradiography experiments were performed at the Department of Neuroscience, Karolinska Institutet. The sectioning took place on a Leica cryomacrocut system. The resulting slices were horizontal brain slices of 100 μm thickness.

The autoradiographic procedures were identical with the former studies done in our laboratory.[15,25] Briefly, 100 μm thick whole hemisphere sections were incubated for 90 min at room temperature with 4 MBq/200 ml of the corresponding radiotracer in 50 mM TRIS buffer pH 7.4 containing sodium chloride (120 mM), potassium chloride (5 mM), calcium chloride (2 mM) and albumin (0.1% w/v). After the incubation, the sections were washed in the same buffer 3 times for 5 min each time at room temperature, briefly dipped in ice cold distilled water, dried and exposed to phosphorimaging plates. Standards were prepared by serial dilution of the radioligand stock solution in assay buffer. The readings were made in a Fujifilm BAS-5000 phosphorimager, using the phosphorimager's Multi Gauge 3.2 image analysis software (Fujifilm).

Blocking experiments were performed with 10 μM L-deprenyl, rasagiline and pirlindol, respectively.

4.20. PET measurements in a cynomolgus monkey

One cynomolgus monkey (*Macaca fascicularis*) (5.45 kg) was supplied by the Astrid Fagraeus Laboratory of the Swedish Institute for Infectious Disease Control (SMI), Solna, Sweden. The study was approved by the Animal Ethics Committee of the Swedish Animal Welfare Agency and was performed according to 'Guidelines for planning, conducting and documenting experimental research' (Dnr 4820/06-600) of the KI as well as the 'Guide for the Care and Use of Laboratory Animals'.[26] Anaesthesia was induced by repeated intramuscular injections of a mixture of ketamine hydrochloride (3.75 mg/kg/h Ketalar® Pfizer) and xylazine hydrochloride (1.5 mg/kg/h Rompun® Vet., Bayer). A device was used to fix the position of the head of the monkey during the PET experiments.[27] Body temperature was maintained by Bair Hugger-Model 505 (Arizant Health Care Inc., MN, USA) and monitored by an oral thermometer. ECG, heart rate, respiratory rate and oxygen saturation were continuously monitored throughout the experiments and blood pressure was monitored every 15 min.

The PET measurement was performed using the High Resolution Research Tomograph (HRRT) (Siemens Molecular Imaging). List-mode data were reconstructed using the ordinary Poisson-3D-ordered subset expectation maximization (OP-3D-OSEM) algorithm, with 10 itterations and 16 subsets including modeling of the point spread function (PSF). The corresponding in-plane resolution with OP-3D-OSEM PSF was 1.5 mm full width at hal F⁻maximum (FWHM) in the center of the field of view (FOV) and 2.4 mm at 10-cm of F⁻center directions.[28] A transmission scan of 6 min using a single ^{137}Cs source was performed immediately before the injection of the radioligand. List-mode data were acquired continuously for 120 min immediately after intravenous injection of [^{18}F]cpd **18**. Images were reconstructed with a series of frames 9×20 s, 3×60 s, 5×180 s, 17×360 s for both radioligands. Brain magnetic resonance imaging was performed in a 1.5-T GE Signa system (General Electric, Milwaukee, WI, USA). A T1 weighted image was obtained for coregistration with PET and delineation of anatomic brain regions. The T1 sequence was a 3D spoiled gradient recalled (SPGR) protocol with the following settings: repetition time (TR) 21 ms, flip angle 35°; FOV 12.8; matrix 256×256x128; 128×1.0 mm slices; 2 NEX. The sequence was optimized for trade-off between a minimum of scanning time and a maximum of spatial resolution and contrast between gray and white matter.

Before delineation of regions of interests (ROIs), the orientation of the brain was spatially normalized by having the high-resolution T1-weighted magnetic resonance images reoriented according to the line defined by the anterior and posterior commissures being parallel to the horizontal plane and the interhemispheric plane being parallel to the sagittal plane. The T1-weigted MR images were then resliced to the resolution of the HRRT PET system, $1.219 \times 1.219 \times 1.219$ mm. The standardized T1-weighted MR images were used as an individual anatomical template for the monkey.

The monkey underwent one study with an iv injection of 168 MBq [^{18}F] cpd **18**. Regions of interest (ROIs) (the whole brain, the striatum, thalamus, cortex and cerebellum) were delineated on the realigned PET image with the reference to the co-registered MRI. Standard uptake value was calculated using the following equation

$$\%\mathrm{SUV} = \frac{\text{Radioactivity Concentration(KBq/mL)}}{\text{Injected radioactivity(MBq)}} / \text{Body weight(Kg)} \times 100$$

4.21. Radiometabolite analysis

A reverse phase HPLC method was used for the determination of the percentages of radioactivity corresponding to unchanged radioligand and radiometabolites during the course of a PET measurement.[29] Venous blood samples (2 mL) were obtained venously from the monkey at 4, 15, 30, 45, 60, 75, 90 and 120 min after injection of **18**. Plasma (0.5 mL) obtained after centrifugation of blood at $2000 \times g$ for 2 min was mixed with acetonitrile (0.7 mL). The supernatant acetonitrile-plasma mixture (1.1 mL) and the precipitate obtained after centrifugation at $2000 \times g$ for 2 min were

counted in a NaI well-counter. The well-counter consists of a NaI crystal (Harshaw, diameter: 38 mm × 50 mm; diameter of the well: 16 mm; depth: 38 mm). The crystal is housed inside a lead shield cylinder with a wall thickness of approx 5 cm. Furthermore the crystal is coupled to a high voltage supply, set to 900 V (Canberra, model 3002), an energy discriminator (Canberra, model 818) and a timer and counter (GE&E Ortec, model 871).

The radio-HPLC system used in the plasma experiments consisted of an interface module (D-7000; Hitachi), a L-7100 pump (Hitachi), an injector (model 7125 with a 1.0 mL loop; Rheodyne) equipped with a μ-Bondapak-C18 column and an absorbance detector (L-7400; 254 nm; Hitachi) in series with a radiation detector (Radiomatic 150TR; Packard) equipped with a PET Flow Cell (600 μL cell). Acetonitrile (A) and phosphoric acid (10 mM) (B) were used as the mobile phase at 6.0 mL/min, according to the following program: 0–10.0 min, (A/B) 15:85 → 65:35 v/v; 10.0–14.0 min, (A/B) 65:35 → 15:85 v/v; 14.0–15.0 min, (C/D) 15:85 v/v. Radioactive peaks eluting from the column were integrated and their areas expressed as a percentage of the sum of the areas of all detected radioactive peaks (decay-corrected). To calculate the recovery of radioactivity from the system, an aliquot (2 mL) of the eluate from the HPLC column was measured for and divided with the amount of total injected radioanalyte.

Acknowledgements

The authors would like to thank all the members of Karolinska Institutet PET centre for assistance in the PET experiments including special thanks to Miklos Toth, Gudrun Nylen, Siv Eriksson, Ryuji Nakao, Arsalan Amir and Guennadi Jogolev for excellent technical assistance and to Bayer Healthcare AG for their support. The research leading to these results has also received funding from the European Union's Seventh Framework Programme (FP7/2007-2013) under grant agreement n° HEALTH-F2-2011-278850 (INMiND).

References and notes

1. Fuller, R. W.; Roush, B. W. *Arch. Int. Pharmacodyn. Ther.* **1972**, *198*, 270.
2. Bach, A. W. J.; Lan, N. C.; Bruke, D. J.; Abell, C. W.; Bembenek, M. E.; Kwan, S. W.; Seeburg, P. H.; Shih, J. C. *FASEB J.* **1988**, *2*, A1733.
3. Andrews, J. M.; Nemeroff, C. B. *Am. J. Med.* **1994**, *97*, S24.
4. Drukarch, B.; van Muiswinkel, F. L. *Biochem. Pharmacol.* **2000**, *59*, 1023.
5. Youdim, M. B. H.; Bakhle, Y. S. *Br. J. Pharmacol.* **2006**, *147*, S287.
6. Fowler, J. S.; Logan, J.; Volkow, N. D.; Wang, G. J.; MacGregor, R. R.; Ding, Y. S. *Methods* **2002**, *27*, 263.
7. Fowler, J. S.; Volkow, N. D.; Wang, G. J.; Pappas, N.; Shea, C.; MacGregor, R. R.; Logan, J. *Adv. Pharmacol.* **1998**, *42*, 304.
8. Bergstrom, M.; Kumlien, E.; Lilja, A.; Tyrefors, N.; Westerberg, G.; Langstrom, B. *Acta Neurol. Scand.* **1998**, *98*, 224.
9. Ishiwata, K.; Ido, T.; Yanai, K.; Kawashima, K.; Miura, Y.; Monma, M.; Watanuki, S.; Takahashi, T.; Iwata, R. *J. Nucl. Med.* **1985**, *26*, 630.
10. Fowler, J. S.; Macgregor, R. R.; Wolf, A. P.; Arnett, C. D.; Dewey, S. L.; Schlyer, D.; Christman, D.; Logan, J.; Smith, M.; Sachs, H.; Aquilonius, S. M.; Bjurling, P.; Halldin, C.; Hartvig, P.; Leenders, K. L.; Lundqvist, H.; Oreland, L.; Stalnacke, C. G.; Langstrom, B. *Science* **1987**, *235*, 481.
11. Hirvonen, J.; Kailajarvi, M.; Haltia, T.; Koskimies, S.; Nagren, K.; Virsu, P.; Oikonen, V.; Sipila, H.; Ruokoniemi, P.; Virtanen, K.; Scheinin, M.; Rinne, J. O. *Clin. Pharmacol. Ther.* **2009**, *85*, 506.
12. Saba, W.; Valette, H.; Peyronneau, M. A.; Bramoulle, Y.; Coulon, C.; Curet, O.; George, P.; Dolle, F.; Bottlaender, M. *Synapse* **2010**, *64*, 61.
13. Plenevaux, A.; Fowler, J. S.; Dewey, S. L.; Wolf, A. P.; Guillaume, M. *Int. J. Rad. Appl. Instrum. A* **1991**, *42*, 121.
14. Mukherjee, J.; Yang, Z. Y.; Lew, R. *Nucl. Med. Biol.* **1999**, *26*, 111.
15. Nag, S.; Lehmann, L.; Heinrich, T.; Thiele, A.; Kettschau, G.; Nakao, R.; Gulyas, B.; Halldin, C. *J. Med. Chem.* **2011**, *54*, 7023.
16. Nag, S.; Lehmann, L.; Kettschau, G.; Heinrich, T.; Thiele, A.; Varrone, A.; Gulyas, B.; Halldin, C. *Bioorg. Med. Chem.* **2012**, *20*, 3065.
17. Bowen, R. D.; Harrison, A. G.; Reiner, E. J. *J. Chem. Soc., Perkin Trans. 2* **1988**, 1009.
18. Couty, F.; Durrat, F.; Prim, D. *Tetrahedron Lett.* **2004**, *45*, 3725.
19. Metro, T. X.; Appenzeller, J.; Pardo, D. G.; Cossy, J. *Org. Lett.* **2006**, *8*, 3509.
20. Nag, S.; Varrone, A.; Toth, M.; Thiele, A.; Kettschau, G.; Heinrich, T.; Lehmann, L.; Halldin, C. *Synapse* **2012**, *66*, 323.
21. Weissbach, H.; Smith, T. E.; Daly, J. W.; Witkop, B.; Udenfriend, S. *J. Biol. Chem.* **1960**, *235*, 1160.
22. Hall, H.; Halldin, C.; Farde, L.; Sedvall, G. *Nucl. Med. Biol.* **1998**, *25*, 715.
23. Schou, M.; Halldin, C.; Pike, V. W.; Mozley, P. D.; Dobson, D.; Innis, R. B.; Farde, L.; Hall, H. *Eur. Neuropsychopharmacol.* **2005**, *15*, 517.
24. Gillberg, P. G.; Jossan, S. S.; Askmark, H.; Aquilonius, S. M. *J. Pharmacol. Methods* **1986**, *15*, 169.
25. Gulyas, B.; Makkai, B.; Kasa, P.; Gulya, K.; Bakota, L.; Varszegi, S.; Beliczai, Z.; Andersson, J.; Csiba, L.; Thiele, A.; Dyrks, T.; Suhara, T.; Suzuki, K.; Higuchi, M.; Halldin, C. *Neurochem. Int.* **2009**, *54*, 28.
26. Clark, J. D.; Gebhart, G. F.; Gonder, J. C.; Keeling, M. E.; Kohn, D. F. *ILAR J.* **1997**, *38*, 41.
27. Karlsson, P.; Farde, L.; Halldin, C.; Swahn, C. G.; Sedvall, G.; Foged, C.; Hansen, K. T.; Skrumsager, B. *Psychopharmacology (Berl)* **1993**, *113*, 149.
28. Varrone, A.; Sjoholm, N.; Eriksson, L.; Gulyas, B.; Halldin, C.; Farde, L. *Eur. J. Nucl. Med. Mol. Imaging* **2009**, *36*, 1639.
29. Halldin C, S. C.-G.; Farde, L.; Sedvall, G. *Radioligand Disposition and Metabolism*; Kluwer Academic Publishers, 1995, p 55.